Biophysical Chemistry, 33 (1989) 161–176
Elsevier

BPC 01352

Growth and electric current loops in plants

Kiyoshi Toko [a], Takanori Fujiyoshi [a], Chikako Tanaka [b], Satoru Iiyama [b], Toshirou Yoshida [a], Kenshi Hayashi [a] and Kaoru Yamafuji [a]

[a] *Department of Electronics, Faculty of Engineering, Kyushu University 36, Fukuoka 812 and* [b] *Department of Home Economics, Women's Junior College of Kinki University, Iizuka 820, Japan*

Received 31 March 1988
Revised manuscript received 12 January 1989
Accepted 19 January 1989

Multicellular system; Electric current; Proton accumulation; Growth; (Plant)

A theory is presented for a relationship between ion accumulation and electric current loops in multicellular systems such as the roots and stems of higher plants. A network of electric circuits shows that the electric current transported across the cell membrane flows between an elongating region and a mature region, not only in roots but also in stems. In roots, ions constituting the extracellular electric current flow in the external aqueous medium, while in stems an electric current of comparable density flows within the epidermal cell wall. Based on this theoretical result, electric isolation between the elongating and mature regions was made in the case of both roots and stems. The speed of growth during the initial stage was greatly decreased due to a change in the distribution of protons around the surfaces of the plant by cutting off the electric current loop. Electrochemical calculation shows that ions are not always accumulated at the efflux site, since the ion distribution is strongly affected by the relation of the magnitudes between the electric field and electric current. The results calculated for the electric potential and pH distributions around the root agree with experimental data.

1. Introduction

Spatial patterns of electric potential and electric current often appear as macroscopic order during the processes of growth and regeneration in both plants and animals. The appearance of an electric current pattern precedes rhizoid formation in the brown alga *Fucus* [1]. Characean species develop alternating bands of acid and alkaline regions along their cell walls under illumination, and localized elongation occurs in acid regions. The electric current flows from the acid to alkaline regions [2–4]. It has long been known that an inhomogeneous electric pattern appears along the surface of the onion root, a typical example of multicellular systems [5,6]. In roots of barley and bean, electric spatial patterns have also been shown to appear with growth [7–9]. While these experimental studies suggest that such patterns play a role in growth, differentiation and morphogenesis [10,11], the detailed mechanism including spontaneous stabilization of electric spatial patterns has remained unelucidated.

A possible approach to the clarification of the mechanism underlying the appearance of electric patterns is to employ nonequilibrium thermodynamic theory taking into account the electrochemistry of the biological systems concerned. It has been shown that, for the appearance of morphogenetic polarity in *Fucus* eggs, the electric spatial pattern associated with the polarity is a self-organized structure arising under far-from-equilibrium conditions [12,13]. Furthermore, the band structure in Characean species is realized cooper-

Correspondence address: K. Toko, Department of Electronics, Faculty of Engineering, Kyushu University 36, Fukuoka 812, Japan.

atively through simultaneous activation and inactivation of molecules of the H^+ pump within the plasmalemma along the cell [2,3,14]. Such a band structure can be interpreted as being of the self-organized [15], i.e., dissipative type [16]. The spontaneous emergence of an electric pattern occurs through a self-organized process of ion flux across the membrane.

In the present paper, we investigate the mechanism of action on the growth process by the electric current formed through the above self-organized process. For this purpose an electric circuit network is useful for expressing the electrophysiological characteristics of a system comprising an elongation and a mature zone. Particularly in plants, the loosening of cell walls via protons is known to be a controlling factor during elongation growth [17,18]. In discussing the growth of plants, therefore, it is necessary to investigate proton accumulation near the cell wall caused by the electric current, which is produced by activated H^+ pumps. However, the connection between the pH and electric current is obscure, since the pH is low in regions of high electric potential near the surface of Characean cells [3], whereas the root has a low pH at the root tip of low surface potential (fig. 1) [8,19].

Thus, the spatial electric pattern in roots and stems of higher plants was first investigated using a model of the electric circuit network. The existence of electric current loops connecting the mature region to the elongation zone was demonstrated not only for the root but also for the stem. Whereas the electric current within a conductive medium was determined for roots [7], it could not be measured for stems, which usually do not grow in conductive medium but in air. Probably for this reason, the suggestion that longitudinal flow of ions within the epidermal cell wall affects the growth has not been proposed for stems. The present theory shows that in stems a considerable amount of electric current can flow longitudinally in the epidermal cell wall.

Secondly, experiments were performed in order to demonstrate that interruption of the electric current loop markedly affects the speed of growth in both roots and stems of higher plants (*Phaseolus chrysanthos, Vigna unguiculata*). Thirdly, it is pointed out from considerations based on electrochemistry that ions are not always accumulated under given conditions but, rather, are depleted at the efflux site, from which the ions are pumped out. Accumulation of protons is shown to depend on the relation of the magnitudes between the electric field and electric current. The results calculated for the pH and electric potential agree with the experimental data demonstrating acidification near the root tip, and furthermore, provide an explanation for the possibility of alkalinization [7] near the elongation zone of roots.

2. Basic experimental data on electric potential and pH

In this section, we describe briefly the basic data on roots that are necessary for the theoretical description. The experimental procedures and results are detailed in our previous reports [8,9,19]. As for stems, the fundamental data on the electric potential will be given explicitly in section 3.

Seeds of a germinating hypogeal plant (azuki bean; *P. chrysanthos*) were allowed to soak for 3 h, and were then sown on moistened filter papers in darkness at $30 \pm 1°$ C. Roots emerged 1 or 2 days later. Roots longer than about 5 cm were used.

The electric potential near the surface along the root was measured by the use of a multi-electrode system [9,19,20]. About 30 pipette electrodes were arranged at 1.5-mm intervals along the root. The electrode tip was located 0.5–1.0 mm from the root surface, care being taken to ensure that direct, mechanical contact with the root surface was avoided. The reference electrode was placed at a distance from the root. The whole apparatus is composed of electrodes as electric sensors, a hand-made circuit for sampling data adequately and a personal computer for processing and arranging the data. One scan over all the electrodes can be performed within 3 s.

The pH near the root surface was measured with a pH electrode (Iwaki Glass, IW202), the tip diameter of which was less than 1 mm.

Fig. 1 shows the surface electric potential, surface pH and growth speed along the root in a

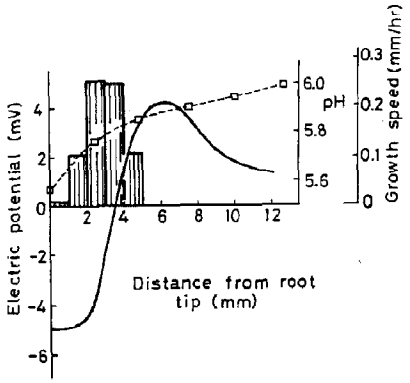

Fig. 1. Properties near the root tip. (———) Electric potential, (□-----□) pH and (bars) growth speed. A root of approx. 8 cm in length was placed in 0.1 mM KCl solution at 30±1°C. Growth speed is averaged over 32 roots longer than 5 cm. The elongating region exists between 1 and 5 mm from tip, where the surface electric potential and pH are relatively low.

narrow region 12.5 mm from the tip. The intact root was placed horizontally in the chamber with 0.1 mM KCl solution. One can see that elongation is limited to 1–5 mm from the root tip while a peak of electric potential exists near 6 mm from the tip. The mature region extends mostly behind approx. 6 mm from the tip. While fig. 1 shows acidification at the root tip and in the elongation zone, alkalinization relative to the elongation zone was sometimes observed close to the root tip. The surface electric potential was low on the side of the tip comprising the elongation zone. On the whole, the pH was high for high surface electric potential under these experimental conditions. The patterns of pH and electric potential disappeared under anoxia [20].

3. Electric circuit network

3.1. Electrophysiological model around the elongating region for roots and stems

There are two independent electromotive forces (e.m.f.) in the radial direction of the electrophysiological structure in the stem as well as the root [21–23]. One is located at the surface of the parenchyma symplast, the other between the parenchyma and xylem. These two kinds of proton pumps work in opposite directions, i.e., back-to-back. Fig. 2 illustrates this situation, which may hold for both the root [23] and stem [21]. In this figure, the symbols x, p and s denote the xylem, parenchyma and surface, respectively. The measured electric potential is represented by V. For example V_{ps} designates the potential at p measured from s. The e.m.f. and electric resistance of the electrogenic pump are given by E_e and r_e, respectively. The e.m.f. of the passive (diffusive) channel is E_d, the resistance being r_d. The additional subscripts 1 and 2 concern the quantities at the plasmalemma of epidermal and cortical cells responsible for the generation of V_{ps} and those at the symplast/xylem interface producing V_{px}, respectively. The parallel resistance due to the Casparian strip, which is an insulating structure against ion and water movement, is so large that it has been omitted as it effectively amounts to infinity. The parenchyma can be regarded as a cytoplasmic continuum [24–27].

Although ions can easily flow in the external aqueous medium in the case of roots, there is no conductive medium in the case of stems, which

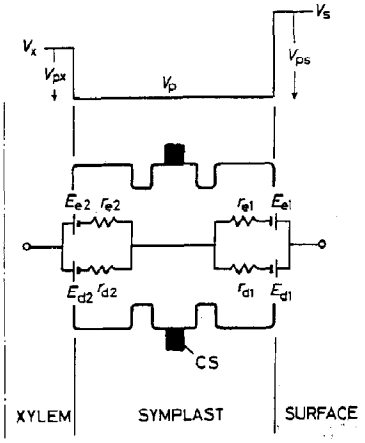

Fig. 2. Electrophysiological structure in the radial direction of the root and stem. CS, Casparian strip. This model is illustrated according to previous electrophysiological studies [21–23]. Subscripts s, p and x to V designate the surface, parenchyma and xylem, respectively. The electrogenic pump is described by the electromotive force E_e and the electric resistance r_e, the diffusion channel being expressed by E_d and r_d. Subscripts 1 and 2 refer to the surface and xylem sides, respectively.

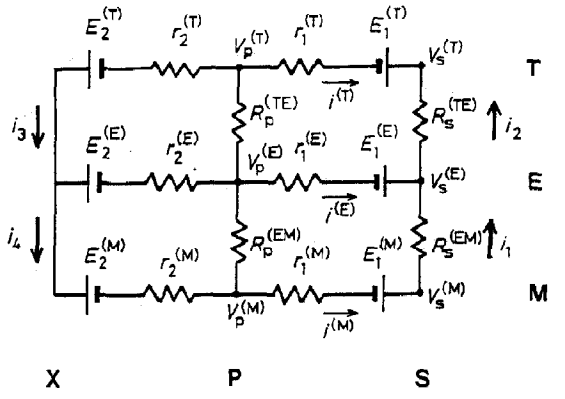

Fig. 3. Electric circuit network model of electrophysiological structures of roots and stems. Tip, elongating and mature regions are indicated by t, e and m, respectively. In the radial direction, the electromotive force is expressed by E with electric resistance r. These are expressed by the electric elements defined in fig. 2. Subscripts denote the radial positions: s, surface; p, parenchyma; x, xylem; 1, surface side; 2, xylem side. Superscripts denote parameters with respect to the longitudinal direction. Note that the electric resistances between the tip and elongating regions are introduced by $R_p^{(te)}$ and $R_s^{(te)}$, together with those between the elongating and mature regions, $R_p^{(em)}$ and $R_s^{(em)}$. The surface refers to the aqueous medium in the case of roots, and the cell wall of epidermal cells for stems. Electric currents flowing in the branch are defined by i_1, i_2, i_3, i_4, $i^{(t)}$, $i^{(e)}$ and $i^{(m)}$.

usually grow in air. However, we can expect the presence of a longitudinal ionic flow even for stems. Ions are able to diffuse not only across the parenchyma symplast but also in the cell wall of the epidermis. In fact, the Characean cell can also develop the acid/alkali pattern when it is suspended in air [28,29]. Here, the electric current can be considered to circulate longitudinally within the cell wall and the protoplasm between the acid and the alkaline regions, although of small magnitude in the cell wall due to the low conductivity. Even in the case of stems, therefore, an electric current can be formed within the epidermal cell wall. We must take into account the longitudinal flow, which is not considered in fig. 2.

Fig. 3 illustrates the electric circuit network, improved so as to express the longitudinal electric connection among the tip (t), elongating (e) and mature (m) regions. In this model E_i and r_i for $i = 1, 2$ are expressed as:

$$E_i = (r_{di}E_{ei} + r_{ei}E_{di})/(r_{di} + r_{ei}),$$
$$r_i = r_{di}r_{ei}/(r_{di} + r_{ei}), \quad (1)$$

with the terms E_{ei}, etc., defined in fig. 2. The longitudinal resistance of the symplast between the tip and elongating regions is denoted by $R_p^{(te)}$, that between the elongating and mature regions being represented by $R_p^{(em)}$. The longitudinal resistances at the surface are given by $R_s^{(te)}$ and $R_s^{(em)}$. Interpretation of R_s requires some caution: In the case of roots, R_s is mainly composed of the resistivity of the surrounding conductive medium. For stems, on the other hand, R_s should express the longitudinal resistance of the apoplast, i.e., the epidermal cell wall. Since the electric potential is homogeneous along and within the xylem [30], the short circuit is drawn at the xylem in fig. 3. The electric current on the longitudinal branch between the elongating and mature regions at the surface is denoted by i_1, and that between the tip and elongating regions by i_2. The radial electric currents across the plasmalemma of the epidermal cell in the tip, elongation and mature regions are designated $i^{(t)}$, $i^{(e)}$ and $i^{(m)}$, respectively.

3.2. Electric current loops formed in radial and longitudinal directions

The electric current flowing in each branch defined in fig. 3 is explicitly given by

$$i_1 = \left(V_s^{(m)} - V_s^{(e)}\right)/R_s^{(em)},$$
$$i_2 = \left(V_s^{(e)} - V_s^{(t)}\right)/R_s^{(te)},$$
$$i_3 = i_2 + \left(V_p^{(e)} - V_p^{(t)}\right)/R_p^{(te)},$$
$$i_4 = i_1 + \left(V_p^{(m)} - V_p^{(e)}\right)/R_p^{(em)}. \quad (2)$$

3.2.1. Roots

We first calculate the electric current in the case of roots. For a root of typical size, we adopt $L^{(te)} = 2.5$ mm as the average distance between the root tip and elongation zone, $L^{(em)} = 8.0$ mm as the distance between the elongation and mature zones, and radius $r = 0.5$ mm for the symplast (fig.

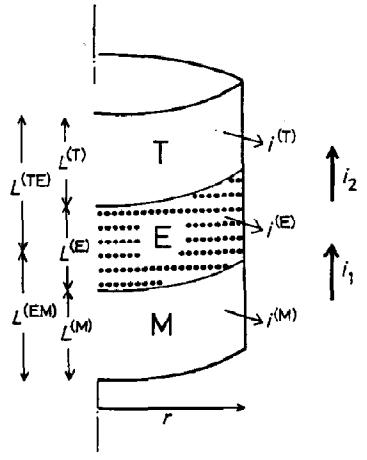

Fig. 4. Definitions of electric currents and lengths. The lengths of the tip, elongating and mature regions are denoted by $L^{(t)}$, $L^{(e)}$ and $L^{(m)}$, respectively. Distances between the two regions are $L^{(te)}$ and $L^{(em)}$ with the radius denoted by r. For roots, $L^{(t)} = 1.25$ mm, $L^{(e)} = 5.25$ mm and $L^{(m)} = 4$ mm; for stems $L^{(t)} = 6$ mm, $L^{(e)} = 18.5$ mm and $L^{(m)} = 12.5$ mm.

4). From fig. 1, the surface electric potentials may be estimated to be $V_s^{(t)} = -5$ mV, $V_s^{(e)} = -4$ mV and $V_s^{(m)} = 2$ mV. The electric potentials in the parenchyma may be evaluated as $V_p^{(t)} = -95$ mV, $V_p^{(e)} = -105$ mV and $V_p^{(m)} = -75$ mV [31]. As for the electric resistance in the longitudinal direction of the parenchyma, we assume the resistivity to be $2.5 \times 10^2 \Omega$ cm [32,33]. Using this value, $R_p^{(te)}$ and $R_p^{(em)}$ can be estimated as 7.96×10^3 and 2.55×10^4 Ω, respectively. The resistivity of the external aqueous medium, e.g., 0.1 mM KCl solution, is approx. 4×10^4 Ω cm. In analogy with the Characean cell [14,15], electric current flows within the cylindrical region of the conductive medium, whose radius is at most 5-times greater than that of the root. The longitudinal resistances $R_s^{(te)}$ and $R_s^{(em)}$ are therefore estimated to be 5.30×10^4 and 1.70×10^5 Ω, respectively.

Substitution of these values into eq. 2 yields the following:

$$\begin{aligned} i_1 &= 3.53 \times 10^{-8} \text{ A } (>0), \\ i_2 &= 1.89 \times 10^{-8} \text{ A } (>0), \\ i_3 &= -1.24 \times 10^{-6} \text{ A } (<0), \\ i_4 &= 1.21 \times 10^{-6} \text{ A } (>0). \end{aligned} \tag{3}$$

The electric current densities in the external conductive medium amount to 0.19 μA/cm^2 between the elongating and mature regions, and 0.10 μA/cm^2 between the tip and elongating regions. These values are consistent with current densities measured by using a vibrating probe [7,34,35]. From the flux continuity, we can also estimate the radial flow across the surface $i^{(t)}$, $i^{(e)}$ and $i^{(m)}$ defined in figs. 3 and 4. These parameters are related to i_1 and i_2 in terms of the current density:

$$\begin{aligned} &i^{(t)} = -i_2/2\pi r L^{(t)}, \; i^{(e)} = (i_2 - i_1)/2\pi r L^{(e)}, \\ &i^{(m)} = i_1/2\pi r L^{(m)}. \end{aligned} \tag{4}$$

We obtain $i^{(t)} = -0.48$ μA/cm^2 (<0), $i^{(e)} = -0.10$ μA/cm^2 (<0) and $i^{(m)} = 0.26$ μA/cm^2 (>0). These values are of comparable order to the longitudinal flux. Fig. 5a illustrates the resultant flow pattern within a region approx. 1 cm in length comprising the tip, elongating and mature regions. Electric current loops are formed in the area including the tip, elongating and mature regions.

We feel that some comments are required concerning this result. The surface electric potential near the root tip is so dynamic that it exhibits large negative values or sometimes relatively positive values. This tendency is evident for roots of shorter length [5,19], the electric current of which is measured via a vibrating probe [7,34,35]. Therefore, the sign and magnitude of i_2 readily undergo change whereas those of i_1 do not. This means that both $i^{(t)}$ and $i^{(e)}$ display considerable variations while $i^{(m)}$ does not. If $V_s^{(t)}$ equals -8 mV,

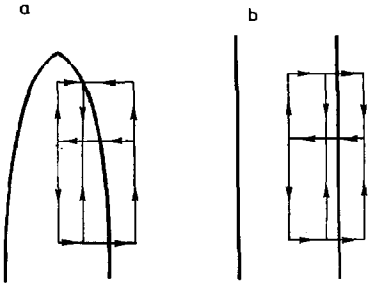

Fig. 5. Theoretical results on electric current loops for root (a) and stem (b). The longitudinal direction is illustrated in the same way as in figs. 3 and 4.

for example, then i_2 amounts to 7.55×10^{-8} A, which leads to $i^{(t)} = -1.92\ \mu A/cm^2$ (< 0) and $i^{(e)} = 0.24\ \mu A/cm^2$ (> 0). In this case, the electric current comprises efflux from the elongation zone as well as from the mature region. Influx occurs only in the tip region. Since a positive peak always appears around 1 cm, located within the mature region for roots of greater length [8,9,19], the mature region behaves as a source of electric current for the external conductive medium.

3.2.2. Stems

Typical values of the dimensions for a stem are as follows: $L^{(te)} = 1.2$ cm, $L^{(em)} = 2.5$ cm and $r = 0.1$ cm. The surface electric potential in each region is $V_s^{(t)} = -5.8$ mV, $V_s^{(e)} = -17.3$ mV and $V_s^{(m)} = 11.4$ mV; the electric potential within the symplast amounts to $V_p^{(t)} = -110.7$ mV, $V_p^{(e)} = -127.2$ mV and $V_p^{(m)} = -117.2$ mV [21]. In the case of stems, if the value adopted for the resistivity of the parenchyma is taken to be the same as that of the root ($= 2.5 \times 10^2\ \Omega$ cm), the values of $R_p^{(te)}$ and $R_p^{(em)}$ may be determined as 9.56×10^3 and $1.99 \times 10^4\ \Omega$, respectively. There is no conductive medium surrounding a stem, but an electric current can flow within the cell wall instead. The longitudinal resistance per unit length of cell wall has been determined to be approx. $10^8\ \Omega$/cm [28,33]. Thus $R_s^{(te)}$ and $R_s^{(em)}$ show values of 1.2×10^8 and $2.5 \times 10^8\ \Omega$, respectively, which are much greater than that of the external conductive medium surrounding the root.

From eq. 2, we obtain

$$\begin{aligned} i_1 &= 1.15 \times 10^{-10}\ \text{A}\ (>0), \\ i_2 &= -9.58 \times 10^{-11}\ \text{A}\ (<0), \\ i_3 &= -1.73 \times 10^{-6}\ \text{A}\ (<0), \\ i_4 &= 5.03 \times 10^{-7}\ \text{A}\ (>0). \end{aligned} \tag{5}$$

This result implies that the magnitude of the electric current flowing within the cell wall is about 0.01% of that flowing in the xylem and also in the symplast. Efflux occurs from the surface side in the mature and tip regions; however, electric current flows into the parenchyma in the elongating region (fig. 5b). Within the xylem current flows downward from the elongating region in the direction of both the tip and mature regions.

The electric current densities can be evaluated as $i_1 = 1.8\ \mu A/cm^2$ (> 0) and $i_2 = -1.5\ \mu A/cm^2$ (< 0) if the thickness of the epidermal cell wall is assumed to be 1 μm. It is noticeable that the above values are comparable to or greater than the current densities flowing around the root in a conductive medium. The density of electric current traversing the plasmalemma of epidermal and cortical cells can be calculated from eq. 4, yielding the values $i^{(t)} = 2.54 \times 10^{-4}\ \mu A/cm^2$ (> 0), $i^{(e)} = -1.82 \times 10^{-4}\ \mu A/cm^2$ (< 0) and $i^{(m)} = 1.46 \times 10^{-4}\ \mu A/cm^2$ (> 0). These values of the radial fluxes are considerably smaller than those of the longitudinal fluxes i_1 and i_2. This occurs because the current must flow longitudinally in the narrow apoplasmic space of epidermal cells, while the radial current is generated across the relatively wide area of the plasmalemma. The resultant flux pattern is illustrated in fig. 5b, the above-mentioned area being composed of the tip (hook part), elongating and mature regions, reaching approx. 4 cm as a whole. Two large loops are formed between the xylem and the surface around the elongating region.

4. Electric isolation

The experimental procedures employed for electric isolation are detailed in appendix A. With roots, the elongating region was electrically isolated from the mature region. The results obtained can be summarized as follows [19]: roots being treated showed slower rates of elongation than the control. The pH displayed lower values in the mature-region side compared to the elongating-region side. In contrast, the pH showed lower values in the elongating region for the control group.

The theoretical result described in section 3 is that an electric current flows longitudinally along a root in the external medium to the tip side. By taking into account the mechanism of acid elongation [17], a straightforward explanation for these results may be given as follows: Protons are transported from the mature-region side to the tip region under the usual conditions, and accumulate in the tip and elongating regions, thus causing wall loosening. Electric isolation inhibited longitu-

dinal ionic flow in the external conductive medium, resulting in depletion of protons in the elongating region; a decrease in the rate of wall loosening resulted, and consequently elongation was retarded.

Fig. 6a concerns electric isolation between the elongating and mature regions in the case of stems. The only difference in experimental details between the electric-isolation and control groups is the difference in shape of the plastic plate, as shown in fig. 10. Stems under electric isolation grew at a lower rate than the control group. The pH in both mature and elongating regions showed higher values for stems under electric isolation compared to the control group, although the pH reflects only qualitatively the pH of the cell wall due to the presence of the cuticle. This result provides an explanation for the slow rate of elongation of stems under isolation, since wall loosening is scarcely able to occur at high pH values. Therefore, we can consider the electric current in the control group to be composed partly of the flow of protons between the elongating and mature regions through the aqueous phase contacting the surface of the stem. Electric isolation interrupts the extracellular current loops. Since both control and electric-isolation groups are in contact with wet filter paper, the difference in growth speed is determined by whether or not electric current loops are formed. The electric loop between the elongation and mature zones is essential. In fact, the cut-off of electric current flowing between different parts of the mature region did not affect the growth of stems (fig. 6b).

In the present experiment, the electric current flowing within the aqueous phase contacting the surface of a stem was interrupted directly. This electric current must flow within the epidermal cell wall under the normal conditions of being wholly surrounded by air, as depicted in fig. 5b;

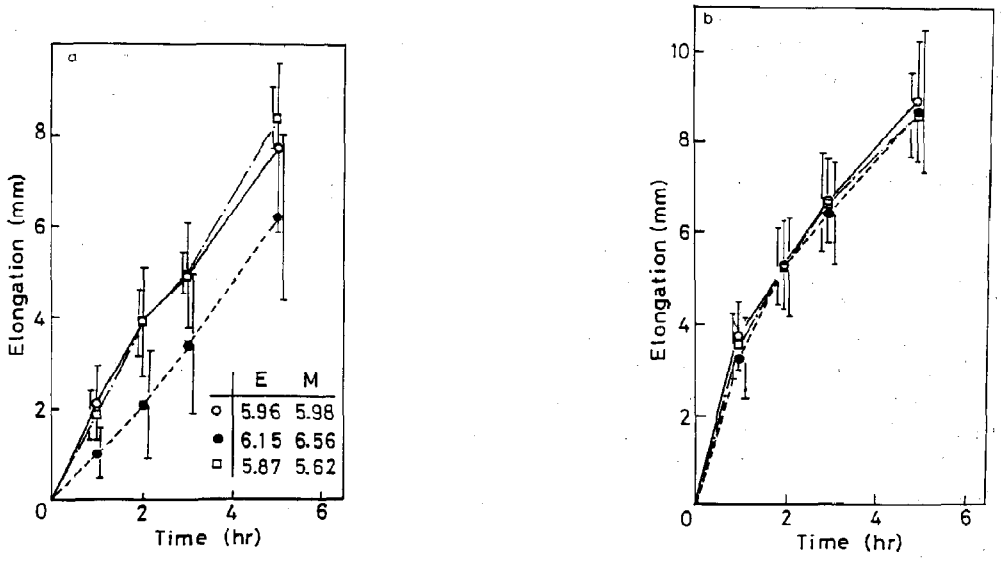

Fig. 6. Experimental results on electric isolation for the stem. Vertical bars represent standard deviations. (Inset) Tabulation of pH value in each region (e, elongating; m, mature region). (○) Control, (●) electric isolation, (□) normal conditions, i.e., stems growing in air free of the attached wet paper. (a) Electric isolation between elongating and mature regions, i.e., at 18 mm from the cotyledonary node. 25, 27 and 18 stems were used at 30 °C for the control, isolation and normal groups, respectively. pH values are those measured 2 h following the start of the experiment, where the respective numbers of stems used were 17, 8 and 13. Among the control eight stems showed almost the same pH values as in the normal group. pH in the elongating and mature regions increased with time in stems under electric isolation. (b) Isolation between mature regions, i.e., at 30 mm from the base at 30 °C. Respective numbers of stems were 19, 22 and 20.

this forms an intra- and extracellular electric current loop together with the flow in the multicellular continuum comprising the symplast and xylem.

In both roots and stems, delay in the rate of growth under electric isolation occurred only during the initial stages. Since the control group was treated in the same way as the group under isolation (figs. 9 and 10), the initial low speed under isolation is not due to the effect of some mechanical perturbation associated with the experimental setup of the plant, but rather results from interruption of the electric current. One reason why complete cessation of growth did not occur may in part be due to incomplete isolation: the surface of the root or stem always became moist even when the moisture was wiped off with filter papers. Another possibility is that partial efflux from the elongating region may occur [19,34–36]. Once the elongating region has changed into the mature region, it becomes a source of electric current, thus giving rise to the usual growth speed.

From the viewpoint of acid elongation of the cell wall, the behavior of protons may be important. Section 5 addresses the question of the electrochemistry for the relationship between ion accumulation and electric field.

5. Ion accumulation and electric field

A one-dimensional system composed of an aqueous solution of $0 < x < L$ containing some ion species is considered here. At the two boundaries, transport of cations (J_i) and of anions (J_k) takes place. The situation is demonstrated in fig. 7. The ion species are limited to monovalent ions. The fluxes j_i for cations ($i = 1, 2, \ldots, m$) and j_k for anions ($k = 1, 2, \ldots, n$) in the medium are explicitly given by

$$j_i = -D_i\,\partial c_i/\partial x + u_i E c_i,$$
$$j_k = -D_k\,\partial c_k/\partial x - u_k E c_k, \qquad (6)$$

where c_i and c_k designate concentrations, D_i and D_k diffusion constants, u_i and u_k electric mobilities and E the electric field in the medium. Subscripts i and k refer to cations and anions, respectively. The electric field E is dependent on x. A

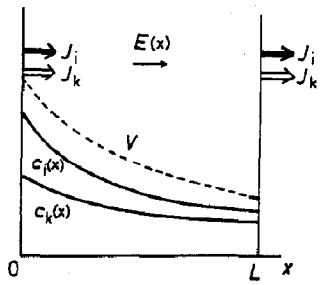

Fig. 7. Concentrations and electric potential in a one-dimensional system with coexisting monovalent cations and anions. Subscripts i ($=1, 2, \ldots, m$) and k ($=1, 2, \ldots, n$) refer to cations and anions, respectively. Fluxes J_i and J_k occur at the two boundaries $x = 0$ and $x = L$. Electric potential V (or electric field E) is determined self-consistently with the distributions of ions.

simple example of the case of constant E is discussed in appendix B.

Concentrations c_i and c_k in the stationary state can be solved easily [37], as shown in appendix C:

$$c_i = \frac{J_i}{Cu_i}c(x) + \frac{AL}{\beta}\left[\bar{c}_i - \frac{J_i}{Cu_i}\bar{c}\right]\left[\left(\bar{c} - \frac{SL}{4\beta}\right)^{1-T/S} - \left(\bar{c} + \frac{SL}{4\beta}\right)^{1-T/S}\right]^{-1} c(x)^{-T/S}, \qquad (7a)$$

$$c_k = -\frac{J_k}{Au_k}c(x) + \frac{CL}{\beta}\left[\bar{c}_k + \frac{J_k}{Au_k}\bar{c}\right]\left[\left(\bar{c} + \frac{SL}{4\beta}\right)^{1+T/S} - \left(\bar{c} - \frac{SL}{4\beta}\right)^{1+T/S}\right]^{-1} c(x)^{T/S}, \qquad (7b)$$

where $c(x)$ is given by

$$c(x) = \bar{c} + \frac{S}{2\beta}\left(\frac{L}{2} - x\right), \qquad (8)$$

with $\bar{c}$ being defined as:

$$\bar{c} = \frac{1}{L}\int_0^L c(x)\,\mathrm{d}x = \sum_{i=1}^{m}\bar{c}_i = \sum_{k=1}^{n}\bar{c}_k. \qquad (9)$$

The quantities C, A, T and S are constants expressed by J_i and J_k; their forms are defined by eqs. C4 and C5. The parameter β is defined by eq.

C2, and is proportional to the absolute temperature, being approx. 25 mV at room temperatures.

The electric field E is given by

$$E(x) = T/2c(x). \tag{10}$$

The potential difference between $x = 0$ and an arbitrary position x is calculated as

$$V(x) = -\int_0^x E(x)\,dx = \frac{\beta T}{S}\ln\left[\frac{\bar{c} + S(L/2 - x)/2\beta}{\bar{c} + SL/4\beta}\right]. \tag{11}$$

If anion transport does not occur at the boundaries or anion flux is negligible compared with cation flux, eqs. 7a and 7b become

$$c_i = \frac{J_i}{Cu_i}c(x) + \frac{SL}{2\beta}\left[\bar{c}_i - \frac{J_i}{Cu_i}\bar{c}\right] / c(x)\ln\left[\frac{\bar{c} + SL/4\beta}{\bar{c} - SL/4\beta}\right], \tag{12a}$$

$$c_k = \bar{c}_k c(x)/\bar{c}. \tag{12b}$$

Eqs. 7, 10, 11 and 12 are the expressions for the concentrations and electric field (or electric potential) in a one-dimensional system where cations and anions are transported across the two boundaries. In roots, ions are transported across the membrane to flow in the aqueous medium. We consider the membranes in the mature and tip-side regions (including the elongating region) as the boundaries at $x = 0$ and L, respectively (fig. 7). The aqueous medium surrounding the root corresponds to the region between $x = 0$ and L.

As major ion species flowing around the root, we deal with H^+, K^+, HCO_3^- and Cl^- by taking account of the experiment of fig. 1. We assume for simplicity that two kinds of cations, H^+ and K^+, are mainly transported across the membrane, since the rate of anion transport is low [38,39]. From the theoretical result (fig. 5a) and the experiment of electric isolation [19], electric current flows from the mature to tip-side region. In the present calculation, the current is composed of H^+ and K^+ and amounts to approx. 0.2 $\mu A/cm^2$ as evaluated from eq. 3 using the electric circuit network. We assume that the largest contribution is that due to K^+, i.e., $J_1 = 0.25$ $\mu A/cm^2$ ($= 2.5$ pmol/cm^2 per s) for K^+ and $J_2 = 2.5 \times 10^{-3}$ $\mu A/cm^2$ ($\simeq 0.025$ pmol/cm^2 per s) for H^+. The value adopted for proton flux is of the same order as that estimated from fig. 1 using the discrete form of eq. 6:

$$J_2 = u_2[H^+][-\beta\,\Delta pH + \Delta V]/l, \tag{13}$$

where u_2 represents the electric mobility of protons ($= 3.626 \times 10^{-3}$ cm^2/V per s), $[H^+]$ proton concentration at the midpoint between the tip and mature regions, i.e., at around 3 mm from the tip, and l ($\simeq 6$ mm) the distance between these regions. ΔpH ($\simeq 0.2$ pH units) and ΔV ($\simeq 9$ mV) denote the respective differences in pH and electric potentials between the two regions.

The calculated results are plotted in fig. 8. The pH profile and electric-potential pattern from 1 to 6 mm agree well with the experimental data in fig. 1: The H^+ concentration is greater and the electric potential lower in the elongating and tip regions compared to the mature region. This tendency is the same as that of case (ii) for $J < uEc_0$ discussed in appendix B (see fig. 11). In fact, this inequality can be easily confirmed by putting $J = J_2$, $u = u_2$, $E = \Delta V/l$ and substituting the value of the proton concentration in the mature region ($\simeq 10^{-5.8}$ M, the value at $x = 0$) for c_0. The present case concerns a strong electric field, since the term comprising E is larger than the flux J. Since the K^+ concentration is greater at the efflux site of high electric potential, the electric field can be considered as being generated mainly by the K^+ flux. Protons are accumulated near the elongating region due to the resultant electric field. The anions, Cl^- and HCO_3^-, are distributed so as to satisfy the requirement of electric neutrality.

The behavior of c_i for H^+ can be easily understood from eq. 12a. The coefficients for the first and second terms are positive. The first term demonstrates that c_i is proportional to $c(x)$, which is nearly equal to the K^+ concentration. The second term signifies that the trend in c_i is opposite to that of $c(x)$. Since $\bar{c}$ and J_i are small, the second term predominates. Thus, the behavior of c_i is the reverse of that shown by $c(x)$, i.e., H^+ is accumulated in the region where K^+ is depleted.

Increasing KCl concentration reduces the electric potential. In this case, the coefficient for the second term in eq. 12a is of negative sign; it

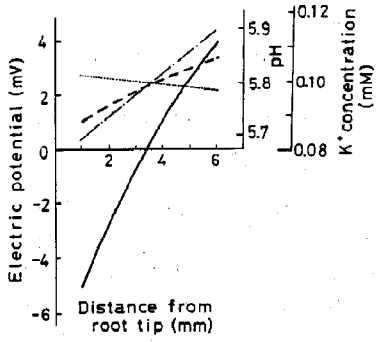

Fig. 8. Theoretical results on electric potential, pH and K^+ concentration near the tip of the root. (———) Electric potential, (- - - - - -) pH and (·—·—·) K^+ concentration near the surface, in 0.1 mM KCl solution. (·····) pH in 1 mM KCl solution. Average pH was set to 5.8. Note that H^+ is accumulated in the elongating region while the K^+ concentration is high in the mature region. Positions 1 and 6 mm from the root tip correspond to $x = L$ (= 5 mm) and $x = 0$ in fig. 7, respectively. Electric potential at $x = 0$ is taken as equal to 4.0 mV. H^+ and K^+ are assumed to be extruded from the $x = 0$ site, i.e., the mature region. The results agree well with fig. 1.

follows that c_i for H^+ shows behavior similar to that of $c(x)$, which is almost equal to the K^+ concentration. Calculation with 1.0 mM KCl, therefore, demonstrated that alkalinization occurred in the elongating region, where the electric current comprises influx, as shown by the dotted line in fig. 8. This provides an explanation for the alkalinization observed previously [7,40]. Protons are accumulated at the efflux site under these conditions, as observed previously in roots and Characean cells [3,35,41].

6. Discussion

The following points have been demonstrated in the present paper:

(1) Theoretical analysis using an electric circuit network suggests the existence of electric current loops formed around the elongating region in both roots and stems. While the current usually flows in the external conductive medium for roots, it occurs within the epidermal cell wall of stems.

(2) Interruption of the surrounding electric current results in the retardation of growth in both the root and stem. This implies a causal relationship between the electric current and the accumulation of protons around the elongation zone on the basis of the acid-growth mechanism [17].

(3) Electrochemical analysis shows that the accumulation of ions is strongly affected by the magnitude of the electric field. Protons are not always accumulated at the efflux site. Theoretical calculation reproduces well the profiles for pH and electric potential in fig. 1. Protons accumulate at the efflux site when the flux is large in relatively high concentrations of coexisting ions, thus explaining the observed data [3,7,35,41].

It has been reported that the value of the pH in the xylem is lowest around the elongating region of stems [21]. This result can be explained theoretically. Fig. 5b provides confirmation that the electric current within the xylem flows downward to both the tip and mature regions from the elongating region. The elongating region is that part which displays efflux within the xylem. The electric-potential difference is known to be zero within the xylem [30], and hence the electric field is zero. This means that the present case falls within the category of weak electric field, i.e., case (i), shown in fig. 11. In this case ions must accumulate around the site of efflux. Thus, the above-mentioned occurrence of the lowest pH values within the xylem around the elongating region is reasonable.

In the present experiment, the cuticle of the stem was not abraded. Many studies have shown that abrasion is necessary for investigation of the quantitative effect of acidification on growth [42–45]. However, ions including protons cannot always pass through the cuticle [46–51]. The cuticle does not behave as an insulator but as a very weak conductor. On a time scale of several tens of minutes, protons can move into and out of a tissue across the cuticle [50]. Since elongation was monitored over a few hours (fig. 6), protons might pass through the cuticle. Slight alkalinization on electric isolation (fig. 6a) may reflect a qualitative pH change in the cell wall resulting from buffering activity of the cell wall [52] and the presence of the cuticle. In addition, the experimental setup might have a favorable effect on the electric connection between the cell wall and medium due to the moist filter paper contacting the stem. A simi-

lar method was also employed in a previous study of the effects of acidification and the geotropic response of hypocotyls [46]; acidification was found to exert a remarkable effect. Furthermore, the effect of intentionally applied acid was not investigated in the present study; however, the effect of a spontaneously formed electric current was studied using electric isolation. In the control group, one may consider that protons can flow according to the electric current even in the presence of the cuticle; electric isolation disturbs this normal process, resulting in the retardation of growth.

Further comment is warranted as regards the difference between the normal and electric-isolation groups, which showed the smaller elongation (fig. 6a). This result appears somewhat uncharacteristic, since the electric current flows within the epidermal cell wall in both cases. A key to resolving this apparent contradiction is provided by the observations made when vaseline was applied around the surface of the stem at a hole while using a plastic shield (fig. 10). This treatment may cause slight penetration by vaseline of the cell wall and/or destruction of the moist layer at the surface of the material, which is always wet. As a consequence, increasing hindrance to ion movement occurs along the organ's surface. A preliminary measurement showed that the electric resistance along the stem increased by approx. 3% when vaseline was spread over the surface at the position separating the elongating from mature region. Since the resistance of the symplast ($\simeq R_p^{(em)}$) may not be altered by this treatment, the small increase in resistance arises from the rise in that of the organ's surface ($\simeq R_s^{(em)} \gg R_p^{(em)}$). Thus, it can be suggested that the longitudinal electric current at the surface is decreased by treatment with vaseline during electric isolation. This leads to less elongation in the electric-isolation group as compared to controls. Since the control group underwent the same treatment, the difference in elongation between control and electric-isolation groups depends on whether or not an electric current loop is formed, connecting the mature and elongating regions through the adjacent aqueous phase, as already mentioned.

Application of auxin aerosol to the stem segment altered the electric potential difference between the parenchyma and organ surface [53]. This experiment does not appear to show a connection between the electric current loops and growth. However, we are certain of the participation of electric current loops in growth under the usual conditions, i.e., in the absence of externally applied stimuli, where growth occurs in the customary manner. If the stem is subjected to a number of stimuli, an overall change, such as a membrane potential, might appear. In this case, proton accumulation occurs firstly at the site of activated pumps, which leads to enhanced elongation, and then the ions undergo redistribution finally, according to the spatial distribution of pump activation. Situations involving such extensive activation due to auxin aerosol may correspond to the weak-field (i.e., strong flux) case, where protons are directly accumulated at the efflux site, resulting in expansion of the wall, as has been observed previously [53].

From the viewpoint of the acid-growth mechanism [17], growth retardation of stems under electric isolation (fig. 6a) can be interpreted as being due to change in pH within the cell wall by cutting off of the electric current between the elongating and mature regions. Another possibility may, however, be considered: the activity of H^+ pumps is altered due to electric isolation, resulting in the cell-wall pH change. This process may be possible because the ion distribution, which may affect activation of the pump, varies according to the electric current. Whereas we are unable to make a definite decision as to which of the two possibilities reflects the true situation, we are able to state unequivocally that the longitudinal electric current constituting the electric loops is necessary for normal growth.

With elongation of the root, a new electric pattern is formed sequentially [19,36]. This process is closely analogous to a mechanism of spacing patterns suggested previously, based on the progress zone [54]. Thus, coupling between elongation and formation of an electric pattern represents a very interesting topic for discussion.

The properties of the electric potential near the root tip are rather dynamic. A small peak or a plateau in the electric potential may be observed

occasionally in the elongating region during growth [19,36]. Spontaneous oscillations are sometimes superimposed on the electric pattern [9]. The behavior of the electric oscillations varies according to the position even over the length of 5 mm limited to the elongation zone (fig. 24 in ref. 19). These results show that the electric properties are not necessarily homogeneous within the elongating region. Furthermore, the electric pattern for young roots readily undergoes change. Protons may be extruded from or sometimes penetrate into part of the elongating region. In addition, with respect to geotropism, the electric-current pattern is drastically changed around the meristem [34]. We can therefore imagine that the electric current loops are dynamically constructed during growth or form in response to external stimuli.

Appendix A

Seeds of a germinating hypogeal plant (azuki bean, *P. chrysanthos*) and an epigeal plant (mitori-sasage, *V. unguiculata*) were allowed to soak for 3 h, subsequently being sown on filter papers with 0.01 mM (or 0.1 mM in fig. 1 for electric measurements in roots) KCl solution in darkness at $30 \pm 1°C$.

The pH at the surface of the hypocotyl was measured by attaching a drop of water to the surface and then placing a pH electrode of diameter 1 mm (Fuji, SE1700GC) at this position for the horizontally oriented stem.

Electric isolation in the longitudinal direction of the root was described in detail previously [19]. A chamber with one thin wall of plastic sheet was utilized for separating the elongation and mature regions, as shown in fig. 9a. The 0.01 mM KCl solution was poured into the chamber so that the root could be submerged. In the control experiment, only a partial mechanical shield was constructed in order to allow electric connection between the two divided regions (fig. 10).

In the case of stems, on the other hand, the hypocotyl elongates in air under normal conditions, i.e., not in an aqueous environment. As shown theoretically, the electric current flows in the epidermal cell wall. As an ideal experiment, therefore, it may be desirable to carry out electric isolation by circumferential deletion of the cell wall at the surface between the elongating and mature regions. However, this treatment in most cases, damaged the hypocotyl organism mechanically. Instead, we attached part of the surface of the hypocotyl to a filter paper moistened with a very small amount of aqueous solution, as shown in fig. 9b. The chamber was oriented vertically in order that the stem could grow upwards, as occurs under normal conditions. In the previous work [36], the system was laid horizontally, a tendency of elongation similar to that shown in fig. 6 being thus obtained. A large part of the surface of the stem is exposed to air. Under such conditions, therefore, the electric current can flow within the epidermal cell wall, and furthermore, escape into the attached aqueous phase. Similarly to the root, isolation was accomplished by means of a plastic shield, with vaseline being applied around the stem in the hole to isolate the two divisions electrically. The experimental condition of the stem being in partial contact with a tiny amount of aqueous

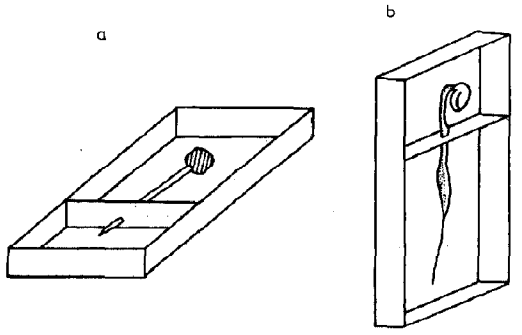

Fig. 9. Experimental setup of electric isolation for roots of *P. chrysanthos* (a) and stems of *V. unguiculata* (b). The root is placed horizontally with the stem being oriented vertically.

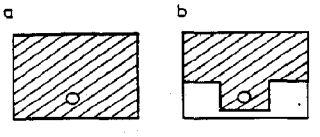

Fig. 10. Shield plates for electric isolation (a) and control (b). Only a partial shield was used for the control so that electric current might flow between the two divisions within the aqueous medium. Vaseline was applied around the hole, into which the root or the stem was inserted.

phase appears to differ somewhat from the normal conditions of growth in air. The stem of the control group, however, exhibited normal growth at almost the same rate of elongation as that of a normal stem (see fig. 6). This means that the present conditions do not represent a close reflection of those pertaining in physiological situations.

Appendix B

For roots, the proton concentration is high in 0.1 mM aqueous KCl solution near the elongating region, where the surface electric potential has a low value, as shown in fig. 1. In Characean cells, on the other hand, protons accumulate near the cell surface where the value of the electric potential is high [3,4]. We attempt here to resolve this apparent contradiction. The problem is tackled with regard to the relationship between ion accumulation and electric field. We shall see that the ion distribution brought about by the ionic flow exhibits two kinds of distinct tendencies according to the coupling with electric potential.

The stationary behavior of monovalent cations is investigated in a one-dimensional system comprising an aqueous solution with $0 < x < L$, where ion transport occurs at the two boundaries $x = 0$, $x = L$ at the rate of flux J. We assume that a homogeneous electric field exists along the x-axis; this implies that the electric potential V changes linearly with distance (fig. 11). The directions of flux J and electric field E are assumed to be the same.

The concentration of the cation species concerned is designated c. The flux j is given by

$$j = -D\,\partial c/\partial x + uEc, \qquad \text{(B1)}$$

where D represents the diffusion constant of the ion, u electric mobility, and E electric field. The first term arises from diffusion, the latter being the electrically driven flux. Concerning the signs of j and E, the x-direction is appointed as positive. By using the elementary charge e (> 0), the electric current density is equal to ej. In the stationary state, flux j must equal the boundary flux J. The stationary concentration c becomes

$$c = J/uE + (c_0 - J/uE)\exp(uEx/D), \qquad \text{(B2)}$$

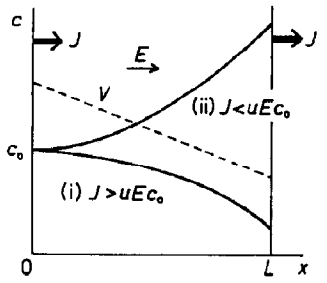

Fig. 11. Concentration and electric potential in the one-dimensional system with a single ion species. Ion concentration is denoted by c and spatial coordinate by x. Electric field E is assumed to be constant. Electric potential V changes linearly with distance. Flux J occurs at the two boundaries $x = 0$ and $x = L$. Cases (i) and (ii) correspond to the weak- and strong-electric-field cases, respectively.

where c_0 denotes the concentration at $x = 0$. Fig. 11 illustrates the variation in c. One can observe from eq. B2 that the distribution of ions is greatly affected by the relative magnitudes of J and E, since the second term changes sign.

When J is greater than uEc_0, the highest value of the concentration occurs near $x = 0$ (case (i) in fig. 11). Ions accumulate at the efflux site when the electric field is weak. The direction of the diffusion flux given by the first term of eq. B1 is the same as that of the electrically driven flux; hence, the total flux j ($= J$) results from the positive contribution by both fluxes.

When J is less than uEc_0, on the other hand, ions accumulate near $x = L$, i.e., near the boundary where influx occurs. This is case (ii) in fig. 11. An intuitive explanation of this result can be made using eq. B1: the diffusion flux (in the direction of negative x) is in balance with the electrically driven flux (in the direction of positive x) under the condition where j ($= J$) is small. In the limiting case, $j = J = 0$, this tendency is most clearly evident. Thus, the condition, $J < uEc_0$, signifies that the situation is close to equilibrium. This phenomenon is analogous to the Hall effect in a semiconductor. Here, electrons (or holes) accumulate at the other end under the influence of a Lorentzian force due to the imposed electric current and magnetic field. At equilibrium, the diffusion flux is in balance with the flux due to the Lorentzian force [55].

Although the electric field is assumed as constant, it must be generated self-consistently through coupling with the ion distribution. The electric potential V decreases with x in this model. In the weak-field case (i) of $J > uEc_0$, it is possible that the decrease in electric potential with x might be due to the flow of ions concerned in this situation. The electric current carried by the ions is necessarily accompanied by a potential drop. In the strong-field case (ii) of $J < uEc_0$, it is difficult for one to suppose that the potential V in fig. 11 stems from the ions concerned. In fact, the distribution of V shows an opposite tendency to that expected from the distribution c, which should evoke a high potential near $x = L$. The potential V can be realized only when the electric potential due to other origins, which produce the decreasing electric potential with x, overcomes the potential due to the ion distribution c. We can therefore suppose that V in case (ii) mainly occurs as a consequence of the ion species differing from those involved in the present situation, provided the electric field is not intentionally imposed on the system from the external circuit.

The result is summarized as follows. Even if the directions of flux and electric field are assumed to be the same, the concentration distribution undergoes variations according to the relative magnitudes of the flux and field. If the effect of the flux is greater than that of the electric field, then cations are accumulated at the efflux site. Under the opposite condition, cations accumulate at the part involved in influx. Here, it is possible that the electric field or electric potential is mostly due to a distribution of other ions. This complicated situation arises from the fact that the electric current is transported by processes expressed as two terms, viz., diffusion flux and electrically driven flux, as pointed out earlier [56].

We now comment upon proton accumulation in the acid region for *Chara*. The origin of the x-axis is chosen as the midpoint of the acid region, in which the surface electric potential has a high value. The electric current is approx. 10 $\mu A/cm^2$ [57] and the electric field strength along the cell is of the order of 25 mV/cm for a change of several millivolts occurring over a few millimeters along the cell [3,41]. Calculation of uEc_0 yields a value of approx. 10^{-14} mol/cm^2 per s with pH ~ 7.0 in the acid region under pH 8.0 buffered. Since the electric current near the acid region can be regarded as being composed mainly of H^+ via H^+ pumping [2,15,29,58], the observed electric current may be compared with uEc_0; this leads to $J \simeq 100$ pmol/cm^2 per s $\gg uEc_0$. This situation belongs in the classification of weak electric field. This signifies that protons accumulate near the efflux site, i.e., in the acid region. Also, in the alkaline region, similar conclusions may be valid for accumulation of OH^-.

In the case of roots, moderate ion concentration with 1 mM KCl being present also leads to classification of this situation as weak electric field. This causes the proton accumulation and depletion at the efflux and influx sites, respectively, which have been observed using a vibrating probe [7,35].

Appendix C

Using Einstein's relation and the stationary conditions $j_i = J_i$ and $j_k = J_k$, eq. 6 can be rewritten as

$$J_i/u_i = -\beta\, \partial c_i/\partial x + Ec_i \quad \text{for } i = 1, 2, \ldots, m,$$
$$J_k/u_k = -\beta\, \partial c_k/\partial x - Ec_k \quad \text{for } k = 1, 2, \ldots, n, \tag{C1}$$

with the definition of β:

$$\beta = k_B T'/e, \tag{C2}$$

where k_B is Boltzmann's constant and T' the absolute temperature.

Electric neutrality is expressed by

$$\sum_{i=1}^{m} c_i = \sum_{k=1}^{n} c_k = c(x). \tag{C3}$$

The quantity $c(x)$ represents the total ion concentration at x. Summation of J_i/u_i in eq. C1 leads to

$$C \equiv \sum_{i=1}^{m} J_i/u_i = -\beta\, \partial c/\partial x + Ec. \tag{C4a}$$

The quantity C denotes the total boundary flux of

cations divided by the electric mobility. This is independent of x. Similarly, we obtain

$$A \equiv -\sum_{k=1}^{n} J_k/u_k = \beta\, \partial c/\partial x + Ec, \qquad \text{(C4b)}$$

where A is a constant relating to the total boundary flux of anions. Its sign becomes positive when the total flow of anions is net influx at $x = 0$ (or efflux at $x = L$), which corresponds to an electric current flowing from $x = 0$ to $x = L$.

Combining eqs. C4a and C4b, we obtain

$$T \equiv C + A = 2Ec. \qquad \text{(C5a)}$$

Eq. C5a implies that the electric field $E(x)$ is of positive sign if the quantity T related to the net electric current is positive. This leads to the potential drop with x. This result is quite reasonable. Subtracting eq. C4a from eq. C4b, we obtain

$$S \equiv C - A = -2\beta\, \partial c/\partial x, \qquad \text{(C5b)}$$

which signifies that the ion concentration near $x = 0$ is high if the total ion flux occurs in the positive x-direction. This result arises from electric neutrality.

Eq. C5b can be easily integrated, since S is a constant composed of the boundary fluxes, and $c(x)$ transforms into eq. 8. Putting $c(x)$ into eq. C5a, we derive $E(x)$. The concentration of each ion species can be calculated from the initial expression, eq. C1, by using $E(x)$. The results are given by eq. 7 or 12.

References

1 R. Nuccitelli and L.F. Jaffe, J. Cell Biol. 64 (1975) 636.
2 D.G. Spear, J.K. Barr and C.E. Barr, J. Gen. Physiol. 54 (1969) 397.
3 N.A. Walker and F.A. Smith, J. Exp. Bot. 28 (1977) 1190.
4 J.-P. Metraux, P.A. Richmond and L. Taiz, Plant Physiol. 65 (1980) 204.
5 E.J. Lund, Bioelectric fields and growth (University of Texas Press, Austin, 1947) p. 123.
6 E.J. Lund, J.N. Pratley and H.F. Rosene, Publ. Inst. Marine Sci. 10 (1965) 221.
7 M.H. Weisenseel, A. Dorn and L.F. Jaffe, Plant Physiol. 64 (1978) 512.
8 S. Iiyama, K. Toko and K. Yamafuji, Biophys. Chem. 21 (1985) 285.
9 K. Toko, K. Hayashi and K. Yamafuji, Trans. IECE Jap. E69 (1986) 485.
10 F.M. Harold, Curr. Top. Membranes Transp. 16 (1982) 485.
11 R.J.P. Williams, J. Theor. Biol. 121 (1986) 1.
12 R. Larter and P. Ortoleva, J. Theor. Biol. 96 (1982) 175.
13 K. Toko and K. Yamafuji, J. Phys. Soc. Jap. 51 (1982) 3049.
14 K. Toko, T. Fujiyoshi, K. Ogata, H. Chosa and K. Yamafuji, Biophys. Chem. 27 (1987) 149.
15 K. Toko, H. Chosa and K. Yamafuji, J. Theor. Biol. 114 (1985) 127.
16 P. Gransdorff and I. Prigogine, Thermodynamic theory of structure, stability and fluctuations (Wiley, London, 1971).
17 D.L. Rayle and R.E. Cleland, Plant Physiol. 46 (1970) 250.
18 J.-M. Versel and G. Mayer, Planta 164 (1985) 96.
19 K. Toko, S. Iiyama, C. Tanaka, K. Hayashi, Ke. Yamafuji and Ka. Yamafuji, Biophys. Chem. 27 (1987) 39.
20 T. Yoshida, K. Hayashi, K. Toko and K. Yamafuji, Ann. Bot. 62 (1988) 497.
21 H. Okamoto, K. Katou and K. Ichino, Plant Cell Physiol. 20 (1979) 103.
22 J.B. Hanson, Plant Physiol. 62 (1978) 402.
23 A.H. de Boer, H.B.A. Prins and P.E. Zanstra, Planta 157 (1983) 259.
24 A.S. Crafts and T.C. Broyer, Am. J. Bot. 25 (1938) 529.
25 W.H. Arisz, Protoplasma 46 (1956) 5.
26 J. Dunlop and D.J.F. Bowling, J. Exp. Bot. 22 (1971) 434.
27 D.J.F. Bowling, Planta 108 (1972) 147.
28 K. Ogata, Plant Cell Physiol. 24 (1983) 695.
29 K. Ogata, K. Toko, T. Fujiyoshi and K. Yamafuji, Biophys. Chem. 26 (1987) 71.
30 K. Ichino, K. Katou and H. Okamoto, Plant Cell Physiol. 14 (1973) 127.
31 H. Ishikawa, K. Yamamura, M. Furukoshi, E. Ohta and M. Sakata, Plant Cell Physiol. 25 (1984) 1045.
32 R.L. Overall and B.E.S. Gunning, Protoplasma 111 (1982) 151.
33 H.M. Behrens and D. Gradmann, Planta 163 (1985) 453.
34 H.M. Behrens, M.H. Weisenseel and A. Sievers, Plant Physiol. 70 (1982) 1079.
35 T. Bjorkman and A.C. Leopald, Plant Physiol. 84 (1987) 841.
36 K. Toko and K. Yamafuji, Ferroelectrics 86 (1988) 269.
37 D.A. MacInnes, The principles of electrochemistry (Reinhold, New York, 1939) p. 461.
38 B.I.H. Scott, H. Gulline and C.K. Pallaghy, Aust. J. Biol. Sci. 21 (1968) 185.
39 M.G. Pitman, Q. Rev. Biophys. 15 (1982) 481.
40 R.A. O'Neill and T.M. Scott, Plant Physiol. 73 (1983) 199.
41 K. Hayashi, T. Fujiyoshi, K. Toko and K. Yamafuji, J. Phys. Soc. Jap. 56 (1987) 810.
42 R. Yamamoto, K. Maki, Y. Yamagata and Y. Masuda, Plant Cell Physiol. 15 (1974) 823.
43 T.J. Mulkey, K.M. Kuzmanoff and M.L. Evans, Planta 152 (1981) 239.

44 L.Z. Wright and D.L. Rayle, Plant Physiol. 69 (1982) 278.
45 A. Mizuno and H. Okamoto, Plant Cell Environ. 5 (1982) 131.
46 S. Iwami and Y. Masuda, Plant Cell Physiol. 14 (1973) 757.
47 S.A. Dreyer, V. Seymour and R.E. Cleland, Plant Physiol. 68 (1981) 664.
48 A.M. Jones and L.N. Vanderhoef, J. Exp. Bot. 32 (1981) 405.
49 R. Prat, M.-B. Gueissaz and R. Goldberg, Plant Cell Physiol. 25 (1984) 1459.
50 R.E. Cleland, D. Cosgrove and M. Tepfer, Planta 170 (1987) 379.
51 L.N. Vanderhoef, J.S. Findley, J.J. Burke and W.E. Blizzard, Plant Physiol. 59 (1977) 1000.
52 S. Ikoma and H. Okamoto, Plant Cell Physiol. 29 (1988) 261.
53 A. Mizuno, K. Katou and H. Okamoto, Plant Cell Physiol. 21 (1980) 395.
54 L. Wolpert and W.D. Stein, in: Pattern formation, A primer in developmental biology, eds. G.M. Malacinski and S.V. Bryant (Macmillan, New York, 1984) p. 3.
55 S. Wang, Solid-state electronics (McGraw-Hill, New York, 1966) p. 152.
56 J.M. Ferrier, J. Theor. Biol. 85 (1980) 739.
57 A. Dorn and M.H. Weisenseel, J. Exp. Bot. 35 (1984) 373.
58 U.-P. Hansen, Ber. Dtsch Bot. Ges. 92 (1985) 105.